Polymer Testing 118 (2023) 107901

Contents lists available at ScienceDirect

Polymer Testing

journal homepage: www.elsevier.com/locate/polytest

# Time, temperature and water aging failure envelope of thermoset polymers

Dennis Gibhardt [a,*,1], Andrey E. Krauklis [b,*,1], Audrius Doblies [a], Abedin Gagani [c], Alisa Sabalina [b], Olesja Starkova [b], Bodo Fiedler [a]

[a] Hamburg University of Technology, Institute of Polymers and Composites, Denickestraße 15, 21073 Hamburg, Germany
[b] University of Latvia, Institute for Mechanics of Materials, Jelgavas Street 3, Riga LV 1004, Latvia
[c] Siemens Digital Industries Software, Via Werner von Siemens 1, 20128 Milano, Italy

ARTICLE INFO

*Keywords:*
Creep
Strength
Composite
Thermo-mechanical behavior
Accelerated testing

ABSTRACT

Epoxies and epoxy-based fiber reinforced polymers (FRP) are significantly affected by environmental impacts during their service life. Exposures to water, humidity, temperature and UV radiation are known to substantially influence the (thermo-) mechanical properties and durability of the materials. Design-relevant characteristics like strength, stiffness, or the glass transition temperature change with time. Therefore, expensive test campaigns are often necessary in advance of a structural design. Prediction models based on physical relations or phenomenological observations are typically required to reduce costs and increase reliability. Consequently, a combined methodology for fast prediction of long-term properties and accelerated aging purposes is presented in this work for a common DGEBA-based epoxy. Therefore, master curves are obtained by creep and constant-strain-rate tests under temperature and moisture impact. A combined time–temperature–water superposition and the Larson–Miller parametrization demonstrate that time-saving CSR tests and modeling can replace long-lasting creep testing. Resulting, the presented methodology allows to determine a polymer's entire (environmental) failure envelope in a relatively short time and with low testing effort.

## 1. Introduction

Epoxy thermosets are widely used as a matrix material in fiber reinforced polymer (FRP) composites [1,2]. Bisphenol A diglycidyl ether (DGEBA) epoxies (used in this work) constitute more than 80 to 85 % of the epoxy market [3]. These materials possess a high specific modulus and strength, low volatility and shrinkage-on-curing, and a relatively high chemical resistance [1,2,4]. Interaction with water often results in both reversible and irreversible effects in epoxy polymers [5–7]. While plasticization is usually reversible (upon redrying), irreversible aging typically occurs due to mechanisms such as oxidation, leaching, physical aging, and post-curing facilitated by water resulting in embrittlement of epoxies [1,8–10]. Epoxies are also strongly affected by the effect of physical aging (relaxation, annealing) that can be amplified by water ingress [10,11].

For the specific studied DGEBA epoxy, it has been reported that it is prone to undergo plasticization [12], hygroscopic swelling [13], and to changes in its viscoelastic properties, when affected by environmental aging [14]. However, it is not being affected by hydrolysis or other chemical degradation [4,12]. Under moderate temperature aging conditions, changes due to thermal oxidation and leaching did not significantly affect the mechanical properties of the investigated epoxy [4,12].

The FRP composite design lifetime in structural applications typically ranges from 20 to 50 years and sometimes spans even longer design lifetimes [15,16]. During this period, the structures are in contact with water, causing deterioration of the mechanical properties [17–19]. Due to the long-spanning design service period, predicting the deterioration of mechanical properties over time is of great interest to the industry for designers and end-users of FRP materials and structures [20–23]. Substantial cost and testing effort savings can be made through efficient use of modeling and simulation tools [21,24]. Typically, developing novel FRPs and their validation is time-consuming and expensive; resources such as time and funding become the bottleneck for composite projects. A benefit would be providing new testing and modeling solutions to the composite market for faster and more efficient processes [25]. A significant percentage of a polymer's development cost is dictated by the decisions made early in the design process. Here, testing is the most time-consuming part of novel FRP product development for the composite industry. Thus, durability prediction methods are seen helpful in reducing the involved costs [7,22,26].

* Corresponding authors.
*E-mail addresses:* dennis.gibhardt@tuhh.de (D. Gibhardt), andykrauklis@gmail.com (A.E. Krauklis).
[1] First authorship is shared as the contribution was equal.

https://doi.org/10.1016/j.polymertesting.2022.107901
Received 5 September 2022; Received in revised form 28 November 2022; Accepted 8 December 2022
Available online 10 December 2022

Accelerated testing methodology (sometimes termed "accelerated degradation tests") are testing programs that are designed to accelerate the property degradation of materials such as polymers and FRPs by subjecting them to conditions outside their normal service range [27,28]. In such methodologies, the degradation is controlled, providing a reliability estimation combined with modeling while reducing the experimental testing time [29,30]. The service lifetime is predicted by modeling the evolution of the critical mechanical characteristics (e.g., strength, stiffness) under controlled accelerated testing conditions, thus establishing safety and reliability criteria [21].

Polymers typically exhibit non-linear and time-dependent behavior that, combined with susceptibility to environmental aging, makes it challenging to model their long-term performance [21]. The mechanical properties of polymers show both a time and temperature dependent viscoelastic behavior [31]. Time–temperature equivalence has been verified for many polymeric systems, such as epoxies. For the thermo-rheologically simple materials [28,29], it is possible to establish temperature functions that enable to translate individual isothermal segments of the chosen response function, e.g., creep compliance, along the time scale and compose a master curve recorded at a reference temperature, $T_{ref}$. This approach is called the time–temperature superposition principle (TTSP), and it allows to extend the time scale beyond the time limits of convenient testing, giving an accelerated testing method.

Prediction methods can be categorized into rate-based (Arrhenius, Eyring, Zhurkov), superposition-based, coupling-based, and parametric models [21]. Each has advantages and disadvantages regarding complexity, information content, and transferability. Therefore, a precise analysis of the boundary conditions and prediction limits is required. The design lifetime of structural composites is practically estimated based on short-term data using predictive models [21]. For instance, Nakada et al. [27] have shown that the long-term viscoelastic behavior of dry epoxies at temperatures below the $T_g$ can be predicted accurately from measuring the 3-hour-short-term creep behavior at elevated temperatures based on the TTSP. Thus, there is a similarity between the effect of water and temperature, as is described by the time–water (moisture, plasticization) superposition principles (TWSP) [32,33]. It was also demonstrated that TTSP and TWSP for dry and wet material can be superimposed, allowing the generation of a single master curve [14]. The $T_g$ can be used as an indicator of polymer chain mobility, as it reduces with increasing water content in epoxies [34–36].

Therefore, this work aims to contribute to developing and promoting modeling and simulation tools and provide a testing methodology that reduces the time needed for testing. A systematic methodology combination was designed and experimentally validated by example of (an amine-cured) epoxy, which allows for long-term property prediction of polymers within a few weeks of testing. An environmental failure envelope for a wide range of operating conditions was developed based on combined time–temperature–water superposition principles, described by Reiner–Weissenberg and Christensen models.

## 2. Materials and methods

### 2.1. Materials

The amine epoxy resin Hexion EPIKOTE™ Resin MGS™ RIMR 135 and the amine hardener EPIKURE™ Curing Agent MGS™ RIMH 137 were investigated, as it is a typical low viscosity system used in various applications like rotor blade and yachting manufacturing. The resin consists chemically of bisphenol A diglycidyl ether (DGEBA) (75 % to 90 %) and 1,6-Hexanediol diglycidyl ether (HDDGE) (10 % to 20 %). The amine hardener consists of Polyoxypropylenediamine (POPA) (50 % to 75 %) and isophorone diamine (IPDA) (25 % to 50 %).

### 2.2. Manufacturing and specimen design

Closed mold RTM processes with thickness defining aluminum frames were used for epoxy plate manufacturing. After degassing using a vacuum stirrer, the epoxy resin was mixed with a ratio of 100:30 parts resin and hardener (by weight). Subsequently, the epoxy was infused with vacuum and held at 50 °C for 10 h. After plate extracting, an additional post-curing process was applied at 80 °C for 16 h, resulting in a complete degree of curing and a $T_g$ of about 90 °C for the dry epoxy. All specimens were machined from the plates using a 1.8 mm diamond mill. For tensile and diffusion tests, dogbone-shaped samples of average thickness of 1.13 mm, length of 150 mm, and width of 10 mm in the parallel part and of 20 mm in the gripping part according to the DIN EN ISO 527-2 1BA standard were used. The specimens dimensions were measured directly before the mechanical test. For aged specimens this was after water absorption occurred. In the case of creep tests, the dogbone-geometry was adapted to 0.5 mm thick, 34 mm long, and 6 mm wide specimens, as described elsewhere by Gibhardt et al. [10], since the DMA setup used is not able to handle the larger specimens. The edges of all specimens were polished with 2500 grit size sandpaper in a defined process of 20 repetitions per side.

### 2.3. Moisture and water absorption

Before testing or hygrothermal aging, all samples were dried in an oven at 60 °C to ensure similar specimen conditions at all involved testing labs. Weight stabilization was achieved within one week, and the amount of desorbed moisture in "as produced" samples was about 0.80 m% after shipment and storage under lab conditions. Dry samples were divided into four groups: three were placed in desiccators under saturated salt solutions of K2CO3, NaCl, K2SO4 giving, at an ambient temperature of 22 °C relative humidity of 43, 75, and 97 % RH, respectively. The remaining part of the samples was immersed in distilled water (DW) at 22 °C.

The moisture or water uptake was detected gravimetrically using a Mettler Toledo XS205 balance with an accuracy of 0.01 mg. The relative moisture or water content $w$ was determined as weight gain per unit weight:

$$w = \frac{(m_t - m_0)}{m_0} \cdot 100, \tag{1}$$

where $m_t$ is the weight of the wet sample at time $t$, and $m_0$ is the weight of the reference (dry) sample. Weight changes were measured using three replicates for each group of samples. The total immersion or conditioning time was 136 days (4.5 months). Mechanical testing of wet aged specimens was performed after 64 days (2 months) of immersion when apparent saturation was reached.

### 2.4. Mechanical tests

Tensile tests were performed using a ZwickRoell Z10 universal testing machine equipped with a 10 kN load cell. To construct a temperature, water, and strain rate-dependent failure envelope, various testing temperatures and strain rates were used. In detail, three testing temperatures 22 °C, 40 °C, and 50 °C, as well as three constant crosshead speeds of 0.1 $^{mm}/_{min}$, 1.0 $^{mm}/_{min}$, and 10.0 $^{mm}/_{min}$ were applied. These correspond to strain rates of $\dot{\epsilon} = 2.8 \cdot 10^{-5}, 2.8 \cdot 10^{-4}$, and $2.8 \cdot 10^{-3}$ $s^{-1}$, respectively. Tensile tests were performed on dry and water- or moisture-saturated samples (five series of samples and three strain rates). The coupled influence of temperature and water was studied on water-saturated samples. The testing temperatures were chosen in consideration of the wet $T_g$ of about 60 °C [10]. Strength values used within this study are always yield strength values.

Tensile creep tests were performed under load control, using a Netsch Gabo Eplexor 500 DMTA equipped with a 500 N load cell and a temperature controlled chamber. The initial strain rate was set to

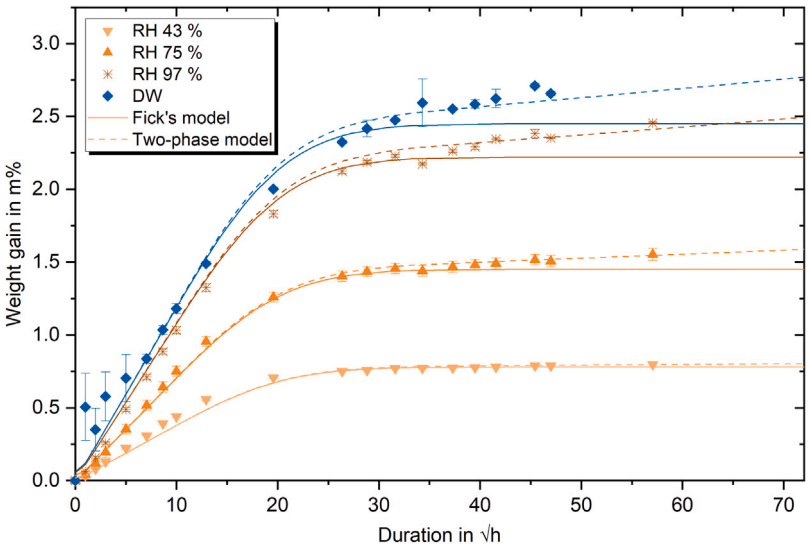


**Fig. 1.** Experimental and modeling weight gain curves of epoxy samples at room temperature (22 °C) exposed in different environments.

1.0 mm/min and the creep stresses were chosen between 85 % and 65 % of the dry and water-saturated strength at each temperature level. These correspond to stresses between 53.0 MPa and 27.2 MPa for the dry and 42.6 MPa and 23.5 MPa for the saturated specimens. After extraction from the aging environments the specimens' free lengths were hand coated using petroleum jelly. The resulting layer serves as a diffusion barrier during the test and prevents the specimens from drying out. Therefore, the re-drying of the specimens was reduced to 0.1 *m%* within 24 h, which is a sixth of the drying of unprotected specimens.

All samples were hold for five minutes in laboratory conditions to achieve thermodynamical equilibrium before testing. Wet samples were tested within five minutes after their removal from water (humid environment). With the exception of the long-term creep tests at low stresses, three replicate samples were tested for each case. In total, 82 CSR and 36 creep tests were performed to build the experimental data base for this study.

## 3. Results and discussion

### 3.1. Water diffusion

The weight gain curves of the epoxy samples exposed to different environments are shown in Fig. 1. One-dimensional diffusion is considered as the dominant mechanism of water absorption in epoxy sheets [7,10,37] (calculations by Fick's model for 1D and 3D cases are demonstrated in the Appendix). At the early stage of water uptake, the epoxy exhibits Fickian-type sorption behavior. All samples reached apparent saturation at $\sqrt{t} \approx 30\,h^{1/2}$, but afterwards a continuous increase of weight changes, typical for two-stage or non-Fickian sorption behavior, is observed. Such deviations from the Fickian sorption are more pronounced at higher water activity and are typically related to water-induced relaxation phenomena in epoxy [7,38–40].

The diffusion–relaxation model of Berens and Hopfenberg was applied to describe the two-stage sorption behavior of the epoxy [38]. According to this model, the diffusion of water in a glassy polymer is contributed by two phenomena: a concentration gradient (Fickian) diffusion and polymer relaxation that contributes by free volume changes and plasticization. Assuming an independent superposition, the total weight $w(t)$ is given as:

$$w(t) = w_d(t) + w_r(t), \tag{2}$$

where subscripts $d$ and $r$ are related to diffusion and relaxation, respectively. The diffusion component in Eq. (2) is given by Fick's equation [41]:

$$w_d(t) = w_{d,\infty}\left[1 - \frac{2}{\pi^2}\sum_{m=1}^{\infty}\frac{(1-(-1)^m)^2}{m^2}\exp\left[-\left(\frac{\pi m}{a}\right)^2 Dt\right]\right], \tag{3}$$

where $D$ is diffusion coefficient and $w_{d,\infty}$ is the equilibrium water content.

The relaxation component in Eq. (2) is expressed by a decaying exponential function related to the polymer relaxation time [38,39]:

$$w_r(t) = w_{r,\infty}\left[1 - \exp\left(\frac{-t}{\tau}\right)\right], \tag{4}$$

where $w_{r,\infty}$ is the equilibrium water content specified by the network relaxation and $\tau$ is the relaxation time.

The approximation results of water absorption curves by Fick's diffusion model and diffusion–relaxation model are shown in Fig. 1. Mechanical tests with wet specimens were performed after $\sqrt{t} = 40\,h^{1/2}$, assuming a homogeneous water distribution in the apparently saturated specimens. The room temperature sorption isotherms for both $w_{d,\infty}$ and $w_{r,\infty}$ are shown in Fig. 2. From the experimental results and the relaxation model can be obtained, e.g., that the maximum water absorption of the epoxy under immersed conditions (sub-$T_g$) will ultimately gain about 3.1 *m%*, which is in line with data based on high temperature accelerated aging presented elsewhere for the same epoxy [10,12]. Furthermore, it is revealed that the long-term maximum water absorption for epoxy resins aged at room temperature or lower temperatures is significantly underestimated when only the Fickian absorption is considered.

### 3.2. Time–temperature–water superposition

Their viscoelastic nature governs the failure of polymers. Thus, methods used for the prediction of viscoelastic properties can also be used for the prediction of the ultimate properties. Miyano et al. [42–44], by the example of various epoxy and vinyl ester-based CFRP and GFRP, validated the use of the time–temperature-superposition principle (TTSP) for several static, creep, and fatigue strengths investigations [42–45]. Similar notes on the construction of master strength curves by TTSP with the same shift functions derived from creep tests are discussed in Guedes et al. [46].

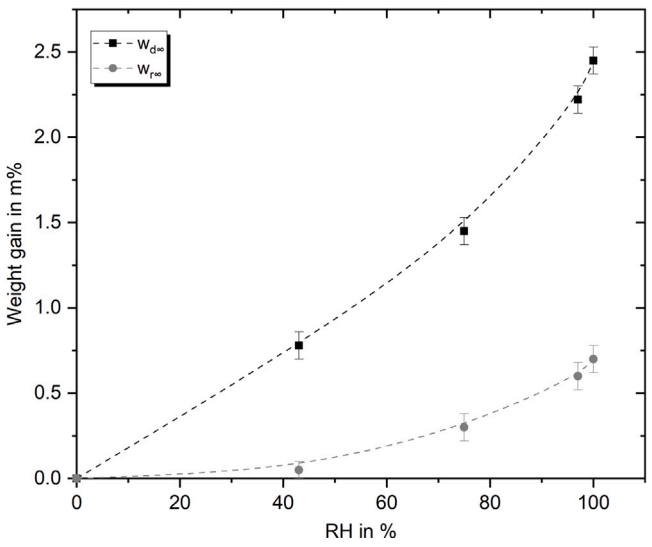


**Fig. 2.** Equilibrium water contents related to the diffusion ($w_{d,\infty}$) and relaxation of the epoxy network ($w_{r,\infty}$).

If a material follows the principle of TTSP [21,29,43], viscoelastic properties, strength in this case, can reach the same values at different time moments (failure times $t_{f0}$ and $t_{f1}$):

$$\sigma(t_{f0}, T_0) = \sigma(t_{f1}, T_1). \tag{5}$$

Here, $\sigma$ can be applied stress in creep tests or rupture stress in CSR tests. Eq. (5) is valid when time and temperature are equivalent and interrelated. This fact allows one to transition to the effective or reduced time by correlating the intrinsic time scale of a material with the observation time. The temperature shift factors $a_T(T)$ are introduced to quantitatively characterize the acceleration of viscoelastic processes, or in other words, the extension of the observation time scale. According to the effective time concept,

$$t_{f0} \times a_T(T_0) = t_{f1} \times a_T(T_1). \tag{6}$$

$a_T$ at the reference temperature $T_0$ is normally taken as unity, $a_T(T_0) = 1$. Then, by taking the equivalence in the logarithmic scale from both sides of Eq. (6) results in

$$\log t_{f0} = \log t_{f1} + \log a_T. \tag{7}$$

It follows from Eqs. (5) and (7) that the strength curves at $T_0$ and $T_1$, when plotted vs. $\log t_f$, are horizontally shifted to each other for the value $\log a_T$. The master curve is obtained by shifting the strength curves for a wide range of temperatures. For glassy polymers at $T < T_g$, the temperature dependence of the shift factor $\log a_T$ is represented by the Arrhenius equation [14,21,43]:

$$\log a_T = -\frac{E_a}{2.303R}\left(\frac{1}{T} - \frac{1}{T_0}\right), \tag{8}$$

where $E_a$ is the activation energy, $R$ is the universal gas constant, and the temperature is taken in Kelvin.

Following analogous discussions, the accelerating effect of absorbed water on the viscoelastic properties of polymers is considered by applying the time–water-superposition principle (TWSP). In this case, the time scale is extended by introducing the time–water shift factor $a_w$ ($w$ is the water or moisture content in a polymer). Under coupled influence of temperature and water, Eq. (5) transforms to:

$$\sigma(t_{f0}, T_0, w_0) = \sigma(t_{f1}, T_1, w_1). \tag{9}$$

Then, assuming additive contributions from both factors, Eq. (7) transforms to

$$\log t_{f0} = \log t_{f1} + \log a_T + \log a_w, \tag{10}$$

i.e., the lifetime is predicted from the sum of single shift functions. In the present study, TTSP and TWSP (and coupled TTWSP) were applied to construct the creep strength (creep failure) and static strength master curves. However, the principles of TTSP, TWSP and TTWSP can only be applied to alike material conditions, which ensure that the model prediction is not affected by chemical or physical changes that will never occur in the reference condition. From this fundamental principal, the assumptions applicable to this study are derived as:

- Uniform water distribution (in saturated samples);
- Plasticization effects are only considered (no degradation, no physical aging);
- Relaxation/physical aging effects (due to water) are insignificant;
- The polymer is in a glassy state ($T < T_g$);
- The same failure mechanism occurs;

### 3.2.1. *Creep-rupture master curves*

Fig. 3 shows the results of the creep tests in terms of applied creep stress versus log failure time. The left part of Fig. 3 displays the acquired results for the different test temperatures of dry and water saturated specimens. Here, it becomes clear that the absorbed water

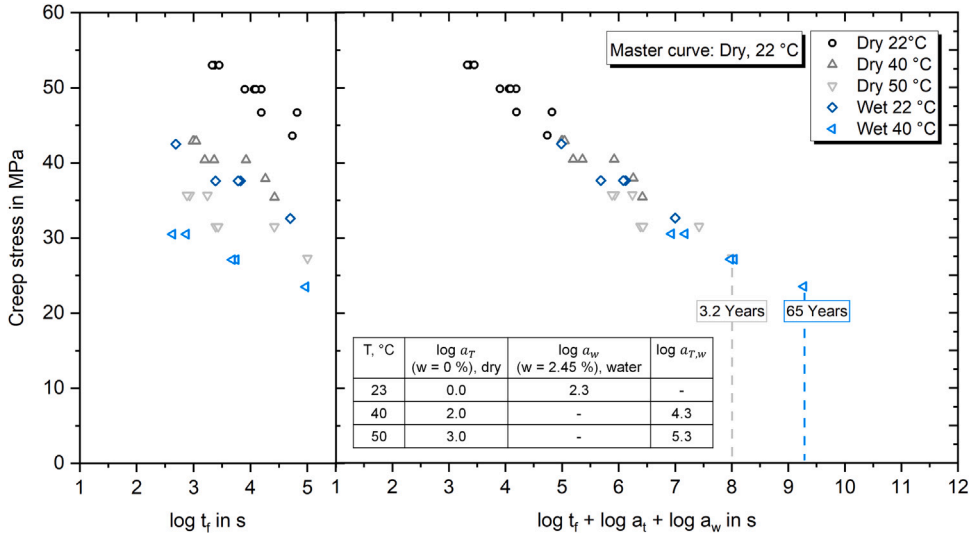


**Fig. 3.** Testing temperature and aging dependent applied tensile stress vs. creep failure time (left) and time–temperature–water-superposition (TTWSP) master curve shift (right).

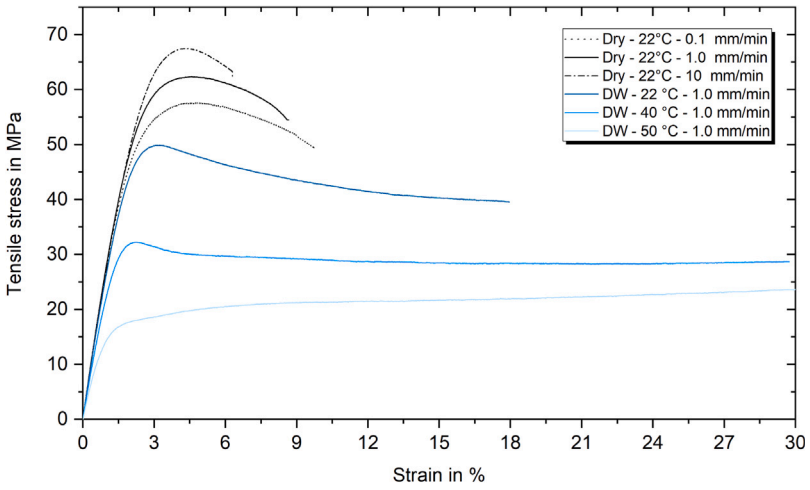


**Fig. 4.** Representative stress–strain diagrams of the different strain rates for dry epoxy specimens and the most important conditions (wet+temperature).

decreases the allowable stress to gain a similar creep lifetime under room temperature conditions in the same dimension as a temperature increase of about 20 °C for dry specimens. This is equivalent to a reduction of the applied stress by about 20 %. For loading of wet epoxy at elevated temperatures of 40 °C, the stresses have to be even halved in order to achieve the same lifetimes as the dry material. In the right part of the Figure, the resulting TTWSP creep master curve is presented together with the temperature, water, and combined shift factors. The temperature shift factors are described by Eq. (8) with $E_a = 196\,\mathrm{kJ/mol}$ ($R^2 = 1$). For any other test temperature, $\log a_T$ can be easily determined with Eq. (8).

As can be taken from the master curve, coupled TTWSP essentially increases the predicted creep lifetime from about three years (dry tests) to 65 years (wet test). At this point, it is essential to mention that all aging procedures were done at room temperature (no temperature-aging effects). The room-temperature methodology ensures a similar and realistic (in the sense of typical applications) contribution of physical aging effects to all tested specimens. It was furthermore validated with hot water conditioning [10,14] that no chemical degradation or chain scission occurs during long-term wet aging. Thus, the authors have ensured that no extra unknown processes were left unaccounted due to temperature effects.

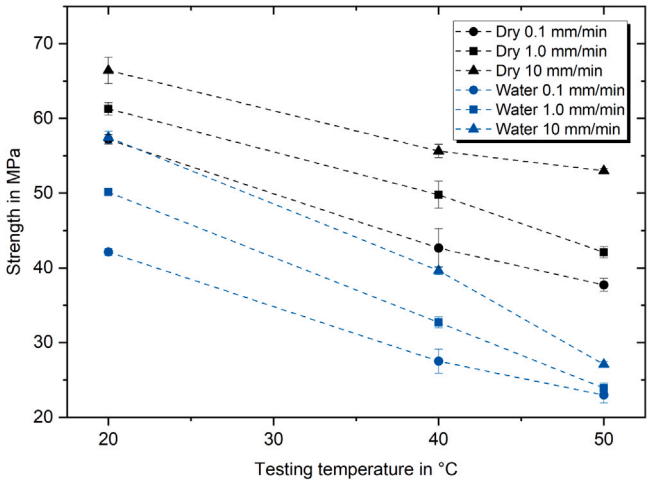


**Fig. 5.** Tensile strength in relation to the testing temperature and strain rate for dry and water saturated epoxy.

### 3.2.2. Static strength master curves

The stress–strain diagrams of the different strain rates for representative dry epoxy specimens and the most important conditions are displayed in Fig. 4. The curves demonstrate both the strength-increasing influence of the higher loading rate and the strength-reducing influence of water and temperature. Strength is defined in the context of the work as the maximum yield stress, which occurs typically between 2.0 % and 5.0 % of strain. By considering all data, it becomes clear that the tests at 50 °C for the water-saturated case, already show fundamental changes. Here, no clear maximum yield stress can be defined in the considered area. Therefore, the stress at the turning point around 8.0 % strain was defined as yield strength for this special condition. The assumptions of including only glassy states and similar failure behaviors are probably no longer completely fulfilled. Consequently, the recommended distance to the (condition-dependent) $T_g$ of at least 20 °C is set as a limitation for the model approach.

Fig. 5 shows the tensile strength (yield strength) dependent on the testing temperature and strain rate for selected conditions. The strength follows an almost linearly decreasing trend with increasing test temperature, which is in line with the behavior of several thermosets investigated in the literature [36,47]. The dry and water-saturated epoxy strength decreases with about $0.8\,MPa/°C$. Therefore, the investigated epoxy is relatively sensitive to temperature effects but is still within a typical range, also reported for other epoxies [36]. The plasticizing effect of water saturation reduces the tensile strength temperature and strain-rate dependent between 10 MPa and 26 MPa. Under room temperature conditions, e.g., the water absorption of 2.6 m% is approximately equivalent to the effect of a temperature increase of about 20 °C.

Furthermore, higher strain rates increase the tensile strength by a nearly constant shift factor. The highest deviations from the linear behavior was observed for the wet saturated specimens tested at an elevated temperature of 50 °C. This behavior is probably due to the proximity between the test temperature and the significantly reduced $T_g$ (about 60 °C according to [10]) in the saturated condition.

The same evaluation and fitting procedure as for creep tests was applied to the CSR tests data and can be seen in Fig. 6. Here, time to failure was taken from the experimental results. Again, the left part of the Figure shows the original experimental data, and the right part displays the master curve, obtained with the same temperature and water shift factors as for the creep tests. This approach shows generally a very good agreement for the CSR data. Nevertheless, the master curve shift also illustrates that the wet 50 °C samples do not fit very well with the remaining. The curve is clearly flattened and the strength underestimated in comparison with dry and wet 40 °C specimens.

CSR tests were also performed with specimens aged and saturated at room temperature at different levels of water activity (different levels

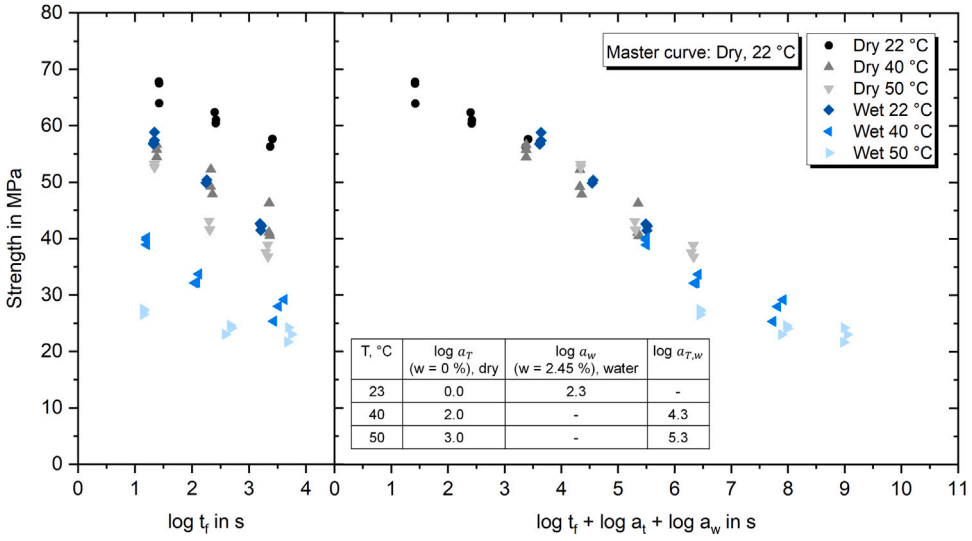


**Fig. 6.** Testing temperature and water dependent constant strain rate (CSR) tensile strength vs. failure time (left). Time–temperature–water-superposition (TTWSP) master curve shift (right).

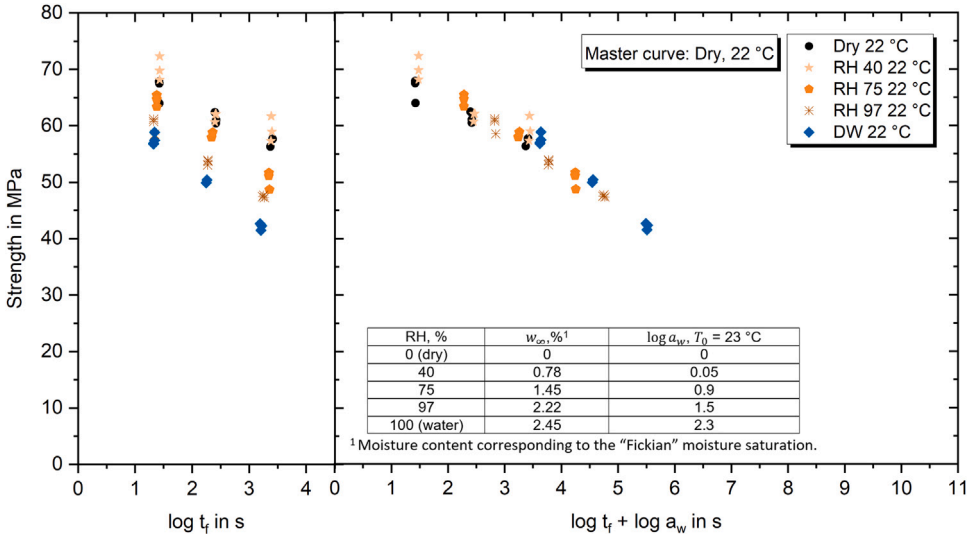


**Fig. 7.** Moisture dependent constant strain rate (CSR) tensile strength vs. failure time (left). Time–moisture-superposition (TMSP) master curve shift (right).

of relative humidity) to extend the findings to a TWSP. The results in Fig. 7 reveal the impact of the environment, and respective water saturation content on the moisture shift factors $\log a_w$. The best fitting solutions suggest an exponential behavior of the shift factors ($\log a_w$) in relation to the relative humidity, as shown in Fig. 8. This is in line with the curves for the maximum amount of absorbed water (Fig. 2) and can be explained by the exponential nature of the polymer–moisture interaction.

### 3.3. Correlation of CSR and creep data

The creep lifetime of epoxy was also modeled by applying the Reiner–Weissenberg (R–W) criterion [29,46,48] to the full data set. According to the R–W approach for time-dependent failure of viscoelastic materials, failure occurs when the stored energy exceeds the limit value that is a material constant. The applicability of TTSP to the R–W energy-based approach is discussed in [49]. The lifetime under constant load for R–W criterion, considering unidirectional creep of linear viscoelastic material, is given as:

$$\left(\frac{t_f}{\tau_0}\right) = \left(\frac{1}{2-2^n}\right)^{\frac{1}{n}} \left(\frac{D_0}{D_1}\right)^{\frac{1}{n}} \left(\frac{1}{\gamma}-1\right)^{\frac{1}{n}}, \text{with } \gamma = \frac{\sigma_0^2}{\sigma_R^2}. \tag{11}$$

Here, $D_0$ is the elastic material constant (compliance) ($D_0 = 1/E$, $E$ is the elastic modulus). $D_1, n$ are viscoelastic material constants, $\tau_0$ is time unity (equal to 1 s in this work, since $t_f$ is measured in seconds). $\sigma_R$ is the strength under instantaneous conditions and $\sigma_0$ is the applied creep stress.

Additionally, another, fracture mechanics based, prediction method developed by Christensen [46,50,51] was applied to the data set. Here, following a kinetic crack formulation, the creep rupture lifetime is found from the time needed for an initial crack to grow to a size critical to cause its instantaneous further propagation. The Christensen criteria for the creep lifetime is given as follows:

$$\left(\frac{t_f}{\tau_0}\right) = \frac{\alpha}{\sqrt{\gamma}}\left(\frac{1}{\sqrt{\gamma}^{1/m}}-1\right), \tag{12}$$

where $\alpha$ and $m$ are material parameters. For both criteria should be mentioned that most of the model parameters must be obtained from the fit of experimental lifetime data [50].

Eqs. (11) and (12) were used to fit the combined experimental creep and CSR strength master curve and both demonstrated good approximation performance, as can be seen in Fig. 9. The model parameters used for calculations are $D_0 = 0.34$ GPa$^{-1}$, $D_1 = 0.08$

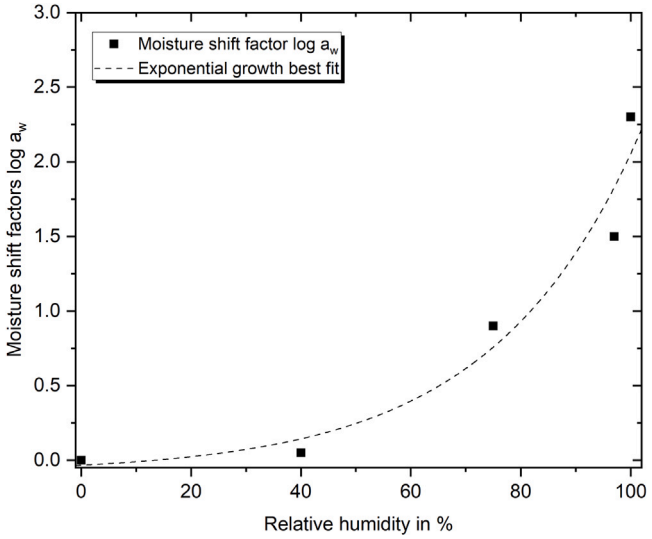


**Fig. 8.** Moisture shift factors $\log a_w$ vs. relative humidity in %. Additionally the best fitting exponential growth function is plotted to guide the eyes.

$GPa^{-1}$, $n = 0.19$, $\alpha = 25$ and $m = 0.07$. As the reference strength under instantaneous conditions, data from CSR tests at 1.0 $\frac{mm}{min}$ were taken. In this way, the two criteria could be successfully applied for the first time to a combined creep/CSR master curve spanning a period of at least 65 years (nearly nine decades) generated with the TTWSP.

Most importantly, it gets evident that the typical creep lifetime in applications with service lives of up to 50 years can be predicted very accurately using time-saving CSR tests only. Deviations between the RW and Christensen model approaches occur mainly for long prediction times of more than four years or high stress loads resulting in lifetimes of less than one hour. However, based on the created data set the Christensen approach fits slightly better especially for long- or short-term predictions. By comparing all results of the combined master curve, it appears that CSR testing does not only enlarge the prediction horizon, it allows to replace time-consuming creep testing. Therefore, the presented TTWSP methodology focusing on CSR testing and inclusion of wet-aged polymers to predict their long-term behavior proves to be an efficient and reliable procedure. As the predictions made from two different types of tests (CSR and creep) and two factors (temperature and water) are in reasonable agreement, their validity is to be assumed. Further validation by means of control tests over several years is hard (costly) to be realized and controlled, and thus is not an effective engineering solution.

Using the creep strength prediction model in combination with the knowledge about the temperature, moisture and combined shift factors, it is possible to predict creep lifetime not only for a reference master curve, but also for any conditions (fulfilling the basic assumptions). As an example, in Fig. 10, the resulting epoxy failure envelope based on the Christensen model fit is shown in a three dimensional space defined by the environmental temperature, the absorbed water content and the time to failure under loading.

The exemplary surfaces shown, are representative for three different load levels. It can be seen that the lifetime is affected by the ambient temperature and simultaneously by the amount of absorbed water. The shown surfaces are based on temperature and moisture shift data equivalent to the tested data set and additional interpolations for testing at 30 °C and/or 90 % RH. In total, each plane in the example is based on 24 data points (15 validated with experimental results). Thus, the entire load-dependent solution space can be spanned. In summary, the presented methodology allows this detailed characterization of individual or combined temperature and moisture effects in a remarkably short time.

### 3.4. Larson–Miller parametrization

Parametric approaches are, in general, methods through which short-term creep-rupture data can be extrapolated using a single time–temperature parameter. The parametrization technique assumes that all creep-rupture data can be superimposed to produce a single master curve of the applied stress vs. a parameter that combines time and temperature [21]. Some methods, such as Larson–Miller parametrization, also allow extrapolation of CSR and fatigue test data. In this work, the Larson–Miller parametrization was applied to predict the lifetime of epoxy based on time, temperature, and water considerations. The Larson–Miller parameter (LMP) is introduced to relate the creep rupture time at different temperatures under given stress [52,53] as:

$$LMP = T(\log t_f + C_{LMP}), \tag{13}$$

where, $T$ is the temperature in Kelvin, $t_f$ is the creep rupture time (here in seconds), and $C_{LMP}$ is a material constant. The Larson–Miller

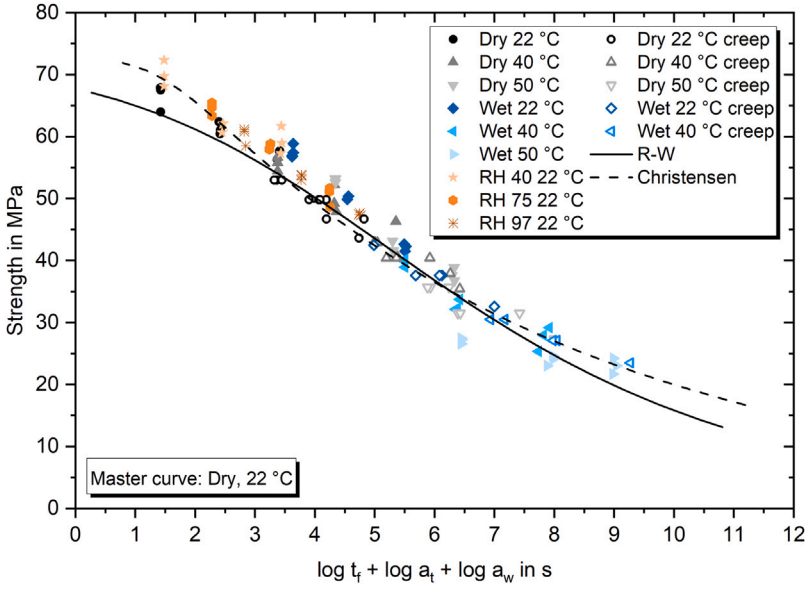


**Fig. 9.** Master curve for combined creep and CSR tests (all data). Additionally R–W and Christensen creep model fittings.

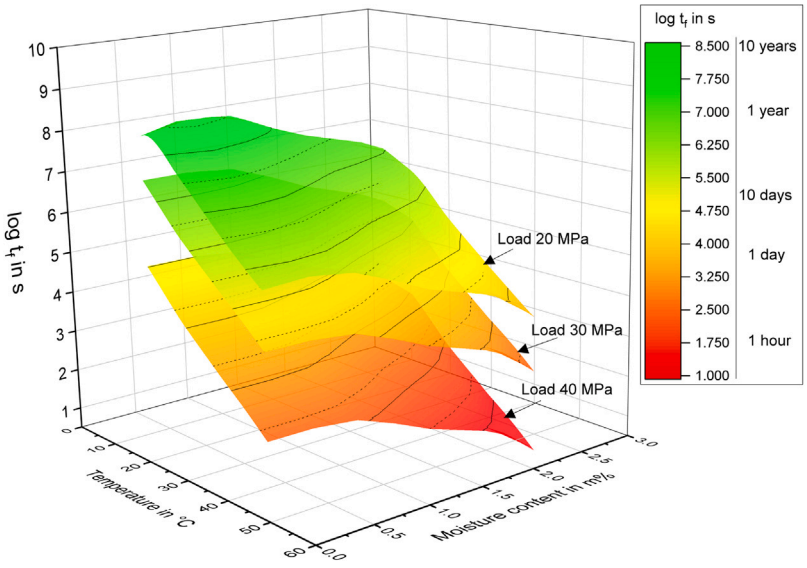


**Fig. 10.** Predicted epoxy failure envelope based on the Christensen model fit in a three dimensional representation.

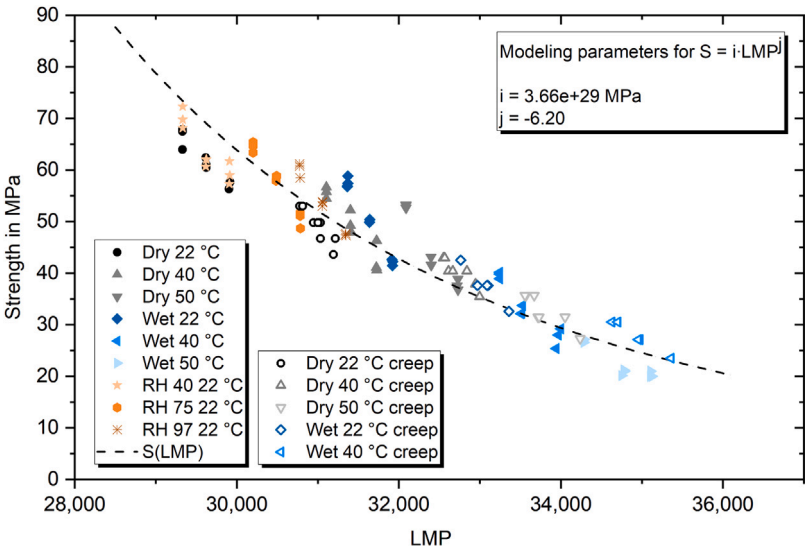


**Fig. 11.** Master curves for creep and CSR strengths according to Larson–Miller parametrization.

constant $C_{LMP}$ is experimentally determined by assuming a linear relationship between the $\log t_f$ versus $1/T$ (Arrhenius relationship) results. Even though $C_{LMP}$ was found to be a material constant for most metallic materials, this may not always be the case with polymers [54]. For the underlying epoxy test data of this work, $C_{LMP}$ is found to be constant for time–temperature considerations across both creep and CSR tests. Still, it is not constant for variations of the epoxy water content. The factor increases with increasing water (moisture) content, as can be taken from Table 1.

Experimental data for tests at different temperatures in the axes stress vs. LMP (calculated with different $C_{LMP}$ for dry and wet specimens) fit well on a common master curve that can be described by a power law function as:

$$S = i(LMP)^j, \tag{14}$$

where $S$ is the creep stress or the rupture stress in the case of the CSR tests, and $i$ and $j$ are fitting parameters. The results of both CSR and creep tests in the LMP-space are shown in Fig. 11. Again, the creep and CSR tests fit well on a single master curve. Therefore, it is demonstrated for the first time that the Larson–Miller parametrization can be successfully used to describe not only temperature but also water (moisture) effects and the combination of both on the mechanical properties of epoxy resins. In comparison with the TTWSP methodology discussed before, the results obtained with the Larson–Miller parametrization show a little more scattering. Tests with different water activities must

**Table 1**
Larson–Miller constant $C_{LMP}$.

| RH in % | $w_\infty$ in m% | $C_{LMP}$ CSR tests | $C_{LMP}$ creep tests |
|---|---|---|---|
| 0 (dry) | 0 | 98 | 101 |
| 40 | 0.78 | 99 | |
| 75 | 1.45 | 101 | |
| 97 | 2.22 | 103 | |
| 100 (water) | 2.45 | 105 | 108 |

verify the Larson–Miller parameter's dependence on water absorption content. Nevertheless, for simpler predictions, checking with room temperature water absorption behavior under immersed conditions is sufficient.

## 4. Conclusion

In summary, this study's combined experimental and modeling procedure delivers reasonable and reliable material characterizations in terms of long-term properties such as lifetime. The combination of TTSP and TWSP modeling was successfully applied to construct the master curves for static strength and creep strength (creep failure times), and most importantly the complete time–temperature–water-stress failure envelope of the epoxy. The master curve is obtained using the same shift factors for both types of tests. The use of coupled TTWSP allowed extending the predicted lifetime for more than two decades and eneables to distinguish between temperature and water effects on the creep lifetime of thermosets. Here, the Reiner–Weissenberg and Christensen criteria were used for the first time to predict the creep lifetime of epoxy based on TTWSP data. Both models well fitted the master curve.

Furthermore, the well-known Larson–Miller parametrization was successfully applied to construct the master curve for the static and creep strengths. The master curve is obtained using the same Larson–Miller parameter $C_{LMP}$ for both types of tests. Water effects are considered by increasing their $C_{LMP}$ values. In future applications, all data can be generated in a short time (about six weeks of test campaign necessary), which is of high importance and significance for the industry, contributing to cost saving and reducing testing time and efforts. Since the presented method was developed on the basis of physical principles, an extension to other thermosets is possible. The requirement is, of course, that these are subject to the model assumptions (e.g. no degradation by water absorption occurs). The slowest and limiting part is the water diffusion or uptake as it is deliberately kept at room temperature. Water absorption curves revealed a two-stage behavior, which could be successfully described with the polymer relaxation processes during aging.

## Funding

This work was funded by the European Regional Development Fund within Activity 1.1.1.2 "Post-doctoral Research Aid" of Specific Aid Objective 1.1.1 of the Operational Programme "Growth and Employment" (Nr.1.1.1.2/VIAA/4/20/606, "Modelling Toolbox for Predicting Long-Term Performance of Structural Polymer Composites under Synergistic Environmental Ageing Conditions").

## CRediT authorship contribution statement

**Dennis Gibhardt:** Conceptualization, Methodology, Investigation, Formal analysis, Investigation, Writing – original draft, Visualization. **Andrey E. Krauklis:** Conceptualization, Methodology, Investigation, Formal analysis, Writing – original draft, Funding acquisition, Project administration. **Audrius Doblies:** Methodology, Investigation. **Abedin Gagani:** Methodology, Writing – review & editing. **Alisa Sabalina:** Investigation. **Olesja Starkova:** Investigation, Formal analysis, Writing – original draft. **Bodo Fiedler:** Methodology , Writing – review & editing, Supervision, Project administration.

## Declaration of competing interest

The authors declare that they have no known competing financial interests or personal relationships that could have appeared to influence the work reported in this paper.

## Data availability

Data will be made available on request.

## Acknowledgments

This work is part of a Postdoctoral Project research funded by the European Regional Development Fund within Activity 1.1.1.2 "Post-doctoral Research Aid" of the Specific Aid Objective 1.1.1 of the Operational Programme "Growth and Employment" (Nr.1.1.1.2/VIAA/4/20/606). Thanks to Anton Akulichev for fruitful discussions on the topic. Andrey is grateful to Oksana.

## Appendix

The fitting procedure for water absorption models by Fick's law and the relaxation model was divided into two steps. First, Eq. (3) was applied to model water diffusion into epoxy up to the apparent saturation $w_{d,\infty}$. The diffusivity was determined from the initial slope of the curve $w$ vs. $\sqrt{t}$, i.e., by using the formula [41]:

$$D = \frac{\pi}{16}\left[\frac{w}{w_{d,\infty}}\frac{1}{\sqrt{t}/a}\right]^2 \tag{15}$$

For the epoxy under study, the diffusivity at room temperature is $D = 6(\pm 0.5)\cdot 10^{-4}\,\frac{\mathrm{mm}^2}{\mathrm{h}}$, and this value is comparable to other types of epoxies [39,55,56]. Next, $\tau$ and $w_{r,\infty}$ were found by fitting the experimental data and providing smooth approximation at longer sorption times. The relaxation time at room temperature conditions (22 °C), being the material characteristic takes the fixed value $\tau = 8.5\cdot 10^3$ h independently of the relative humidity of the environment. The higher $\tau$ is, the more time is required for complete structural rearrangement of the polymer network. This depends on the material, curing degree, and test temperature [10,11,39,57]. Relaxation times determined in water absorption tests correlate well with those determined by alternative methods, e.g., creep tests [58,59] or tensile tests [10,11,60]. The water absorption capacity generally increases with water activity (relative humidity of the environment).

In a general 3D case for an isotropic material the water content $w(t)$ according to the Fick's model is given by the formula [7,41]:

$$w(t) = w_{d,\infty} - \frac{8w_{d,\infty}}{\pi^6}\sum_{k=1}^{\infty}\sum_{n=1}^{\infty}\sum_{m=1}^{\infty}\frac{[1-(-1)^k]^2[1-(-1)^n]^2[1-(-1)^m]^2}{k^2n^2m^2}\exp\left(-\lambda_{k,n,m}^2 Dt\right), \tag{16}$$

where $w_{d,\infty}$ is the equilibrium water content and $\lambda_{k,n,m}^2 = \lambda_k^2+\lambda_n^2+\lambda_m^2 = \left(\frac{\pi k}{a}\right)^2+\left(\frac{\pi n}{b}\right)^2+\left(\frac{\pi m}{l}\right)^2$. For a 1D diffusion problem, when the sample dimensions in one of the directions are significantly smaller than in two others, i.e., $a \ll b, l$, Eq. (16) is simplified to the following equation:

$$w(t) = w_{d,\infty}\left[1-\frac{2}{\pi^2}\sum_{k=1}^{\infty}\frac{(1-(-1)^k)^2}{k^2}\exp\left[-\left(\frac{\pi k}{a}\right)^2 Dt\right]\right], \tag{17}$$

Eqs. (16) and (17) were used for the calculation of water contents in a plate of 1.13 mm thickness ($a$) and 150 mm length ($l$). These are the actual sizes of the epoxy samples under study. In calculations, the width ($b$) of a plate varied from 2 to 20 mm (actual width of samples was 10 mm in the parallel part and 20 mm in the grip zone). The results of calculations are demonstrated in Fig. 12. For given parameters and sample dimensions, differences in 1D and 3D calculations are negligible at $b \geq 10$ mm. Thus, the use of 1D models for the analysis of water absorption is justified within the present study.

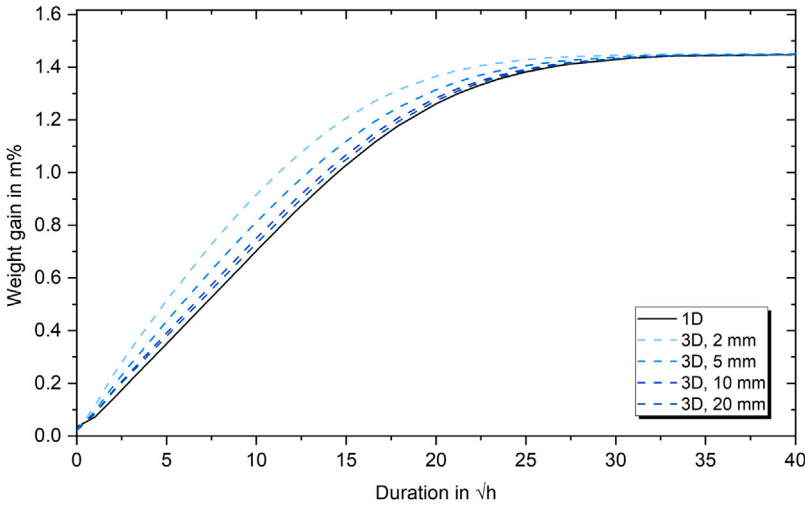


**Fig. 12.** Calculations by Fick's model for 1D and 3D cases for plates of different widths; $l$ = 150 mm, $a$ = 1.13 mm (actual sizes of epoxy samples). $D$ and $w_{d,\infty}$ were taken for 75 % RH.

## References


[1] G.Z. Xiao, M. Shanahan, Swelling of DGEBA/DDA epoxy resin during hygrothermal ageing, Polymer 39 (14) (1998) 3253–3260, http://dx.doi.org/10.1016/S0032-3861(97)10060-X.

[2] A. Toscano, G. Pitarresi, M. Scafidi, M. Di Filippo, G. Spadaro, S. Alessi, Water diffusion and swelling stresses in highly crosslinked epoxy matrices, Polym. Degrad. Stab. 133 (1) (2016) 255–263, http://dx.doi.org/10.1016/j.polymdegradstab.2016.09.004.

[3] N. Karak, Sustainable Epoxy Thermosets and Nanocomposites, Vol. 1385, American Chemical Society, Washington, DC, 2021, http://dx.doi.org/10.1021/bk-2021-1385.

[4] A.E. Krauklis, A.T. Echtermeyer, Mechanism of yellowing: Carbonyl formation during hygrothermal aging in a common amine epoxy, Polymers 10 (9) (2018) http://dx.doi.org/10.3390/polym10091017.

[5] M. Wang, X. Xu, J. Ji, Y. Yang, J. Shen, M. Ye, The hygrothermal aging process and mechanism of the novolac epoxy resin, Composites B 107 (5) (2016) 1–8, http://dx.doi.org/10.1016/j.compositesb.2016.09.067.

[6] T.C. Clancy, S. Frankland, J.A. Hinkley, T.S. Gates, Molecular modeling for calculation of mechanical properties of epoxies with moisture ingress, Polymer 50 (12) (2009) 2736–2742, http://dx.doi.org/10.1016/j.polymer.2009.04.021.

[7] A.E. Krauklis, C.W. Karl, I.B.C.M. Rocha, J. Burlakovs, R. Ozola-Davidane, A.I. Gagani, O. Starkova, Modelling of environmental ageing of polymers and polymer composites-modular and multiscale methods, Polymers 14 (1) (2022) http://dx.doi.org/10.3390/polym14010216.

[8] A.E. Krauklis, Environmental Aging of Constituent Materials in Fiber-Reinforced Polymer Composites (Ph.D. Thesis), NTNU, Trondheim, 2019.

[9] O. Starkova, S. Gaidukovs, O. Platnieks, A. Barkane, K. Garkusina, E. Palitis, L. Grase, Water absorption and hydrothermal ageing of epoxy adhesives reinforced with amino-functionalized graphene oxide nanoparticles, Polym. Degrad. Stab. 191 (17) (2021) 109670, http://dx.doi.org/10.1016/j.polymdegradstab.2021.109670.

[10] D. Gibhardt, C. Buggisch, D. Meyer, B. Fiedler, Hygrothermal aging history of amine-epoxy resins: Effects on thermo-mechanical properties, Front. Mater. 9 (2022) 2544, http://dx.doi.org/10.3389/fmats.2022.826076.

[11] A. Le Guen-Geffroy, P.-Y. Le Gac, B. Habert, P. Davies, Physical ageing of epoxy in a wet environment: Coupling between plasticization and physical ageing, Polym. Degrad. Stab. 168 (2019) 108947, http://dx.doi.org/10.1016/j.polymdegradstab.2019.108947.

[12] A.E. Krauklis, A.I. Gagani, A.T. Echtermeyer, Hygrothermal aging of amine epoxy: Reversible static and fatigue properties, Open Eng. 8 (1) (2018) 447–454, http://dx.doi.org/10.1515/eng-2018-0050.

[13] A. Krauklis, A. Gagani, A. Echtermeyer, Prediction of orthotropic hygroscopic swelling of fiber-reinforced composites from isotropic swelling of matrix polymer, J. Compos. Sci. 3 (1) (2019) 10, http://dx.doi.org/10.3390/jcs3010010.

[14] A.E. Krauklis, A.G. Akulichev, A.I. Gagani, A.T. Echtermeyer, Time-temperature-plasticization superposition principle: Predicting creep of a plasticized epoxy, Polymers 11 (11) (2019) http://dx.doi.org/10.3390/polym11111848.

[15] D. McGeorge, A.T. Echtermeyer, K.H. Leong, B. Melve, M. Robinson, K.P. Fischer, Repair of floating offshore units using bonded fibre composite materials, Composites A 40 (9) (2009) 1364–1380, http://dx.doi.org/10.1016/j.compositesa.2009.01.015.

[16] I. Grabovac, D. Whittaker, Application of bonded composites in the repair of ships structures – A 15-year service experience, Composites A 40 (9) (2009) 1381–1398, http://dx.doi.org/10.1016/j.compositesa.2008.11.006.

[17] D. Gibhardt, C. Fleschhut, B. Fiedler, The influence of different glass fiber/epoxy matrix combinations on the durability under severe moisture impact, Compos. Struct. 942 (1) (2020) 012009, http://dx.doi.org/10.1088/1757-899X/942/1/012009.

[18] V.O. Startsev, M.P. Lebedev, K.A. Khrulev, M.V. Molokov, A.S. Frolov, T.A. Nizina, Effect of outdoor exposure on the moisture diffusion and mechanical properties of epoxy polymers, Polym. Test. 65 (2018) 281–296, http://dx.doi.org/10.1016/j.polymertesting.2017.12.007.

[19] I. Rocha, S. Raijmaekers, R. Nijssen, F.P. van der Meer, L.J. Sluys, Hygrothermal ageing behaviour of a glass/epoxy composite used in wind turbine blades, Compos. Struct. 174 (9) (2017) 110–122, http://dx.doi.org/10.1016/j.compstruct.2017.04.028.

[20] D. Gibhardt, A. Doblies, L. Meyer, B. Fiedler, Effects of hygrothermal ageing on the interphase, fatigue, and mechanical properties of glass fibre reinforced epoxy, Fibers 7 (6) (2019) 55, http://dx.doi.org/10.3390/fib7060055.

[21] O. Starkova, A.I. Gagani, C.W. Karl, I.B.C.M. Rocha, J. Burlakovs, A.E. Krauklis, Modelling of environmental ageing of polymers and polymer composites-durability prediction methods, Polymers 14 (5) (2022) http://dx.doi.org/10.3390/polym14050907.

[22] M. Bruyneel, P. Jetteur, J.P. Delsemme, S. Siavoshani, A. Cheruet, Modeling and Simulating Progressive Failure in Composite Structures for Automotive Applications, SAE Technical Paper Series, SAE International400 Commonwealth Drive, Warrendale, PA, United States, 2014, http://dx.doi.org/10.4271/2014-01-0962.

[23] A. Krauklis, A. Gagani, A.T. Echtermeyer, Long-term hydrolytic degradation of the sizing-rich composite interphase, Coatings 9 (4) (2019) 263, http://dx.doi.org/10.3390/coatings9040263.

[24] M.K. Hagnell, S. Kumaraswamy, T. Nyman, M. Åkermo, From aviation to automotive - A study on material selection and its implication on cost and weight efficient structural composite and sandwich designs, Heliyon 6 (3) (2020) e03716, http://dx.doi.org/10.1016/j.heliyon.2020.e03716.

[25] A.T. Echtermeyer, A. Gagani, A. Krauklis, T. Mazan, Multiscale modelling of environmental degradation—First steps, in: P. Davies, Y.D. Rajapakse (Eds.), Durability of Composites in a Marine Environment, Vol. 2, in: Solid Mechanics and Its Applications, vol. 245, Springer International Publishing, Cham, 2018, pp. 135–149, http://dx.doi.org/10.1007/978-3-319-65145-3_8.

[26] A. Arteiro, G. Catalanotti, J. Reinoso, P. Linde, P.P. Camanho, Simulation of the mechanical response of thin-ply composites: From computational micro-mechanics to structural analysis, Arch. Comput. Methods Eng. 26 (5) (2019) 1445–1487, http://dx.doi.org/10.1007/s11831-018-9291-2.

[27] M. Nakada, Y. Miyano, H. Cai, M. Kasamori, Prediction of long-term viscoelastic behavior of amorphous resin based on the time-temperature superposition principle, Mech. Time-Dependent Mater. 15 (3) (2011) 309–316, http://dx.doi.org/10.1007/s11043-011-9139-8.

[28] I. Emri, Rheology of solid polymers, Rheol. Rev. (2005).

[29] H.F. Brinson, L.C. Brinson, Polymer Engineering Science and Viscoelasticity: An Introduction, 2nd ed. 2015, Springer US, New York, NY, 2015.

[30] M.L. Williams, R.F. Landel, J.D. Ferry, The temperature dependence of relaxation mechanisms in amorphous polymers and other glass-forming liquids, J. Am. Chem. Soc. 77 (14) (1955) 3701–3707, http://dx.doi.org/10.1021/ja01619a008.

[31] H. Cai, M. Nakada, Y. Miyano, Simplified determination of long-term viscoelastic behavior of amorphous resin, Mech. Time-Dependent Mater. 17 (1) (2013) 137–146, http://dx.doi.org/10.1007/s11043-012-9174-0.
[32] V. Fabre, G. Quandalle, N. Billon, S. Cantournet, Time-temperature-water content equivalence on dynamic mechanical response of polyamide 6,6, Polymer 137 (2018) 22–29, http://dx.doi.org/10.1016/j.polymer.2017.10.067.
[33] F. Huber, H. Etschmaier, H. Walter, G. Urstöger, P. Hadley, A time–temperature–moisture concentration superposition principle that describes the relaxation behavior of epoxide molding compounds for microelectronics packaging, Int. J. Polym. Anal. Charact. 25 (6) (2020) 467–478, http://dx.doi.org/10.1080/1023666X.2020.1807680.
[34] B.C. Hancock, G. Zografi, The relationship between the glass transition temperature and the water content of amorphous pharmaceutical solids, Pharm. Res. 11 (4) (1994) 471–477, http://dx.doi.org/10.1023/A:1018941810744.
[35] P.P. Simon, H.J. Ploehn, Modeling the effect of plasticizer on the viscoelastic response of crosslinked polymers using the tube-junction model, J. Rheol. 44 (2) (2000) 169–183, http://dx.doi.org/10.1122/1.551082.
[36] J. Drummer, D. Gibhardt, J. Körbelin, B. Fiedler, General influence of the environmental temperature on the matrix strength under tensile and compressive loading - A comprehensive study on high performance matrices, Compos. Sci. Technol. 39 (4) (2022) 109486, http://dx.doi.org/10.1016/j.compscitech.2022.109486.
[37] J. Zhou, J.P. Lucas, Hygrothermal effects of epoxy resin. Part I: The nature of water in epoxy, Polymer 40 (20) (1999) 5505–5512, http://dx.doi.org/10.1016/S0032-3861(98)00790-3.
[38] A. Berens, H. Hopfenberg, Diffusion and relaxation in glassy polymer powders: 2. Separation of diffusion and relaxation parameters, Polymer 19 (5) (1978) 489–496, http://dx.doi.org/10.1016/0032-3861(78)90269-0.
[39] O. Starkova, S. Chandrasekaran, T. Schnoor, J. Sevcenko, K. Schulte, Anomalous water diffusion in epoxy/carbon nanoparticle composites, Polym. Degrad. Stab. 164 (2019) 127–135, http://dx.doi.org/10.1016/j.polymdegradstab.2019.04.010.
[40] L.-R. Bao, A.F. Yee, C.Y.-C. Lee, Moisture absorption and hygrothermal aging in a bismaleimide resin, Polymer 42 (17) (2001) 7327–7333, http://dx.doi.org/10.1016/S0032-3861(01)00238-5.
[41] J. Crank, The mathematics of diffusion, second ed., reprinted., Oxford science publications, Oxford Univ. Press, Oxford, 2009.
[42] Y. Miyano, M. Nakada, N. Sekine, Accelerated testing for long-term durability of GFRP laminates for marine use, Composites B 35 (6–8) (2004) 497–502, http://dx.doi.org/10.1016/j.compositesb.2003.11.006.
[43] Y. Miyano, M. Nakada, Accelerated testing methodology for durability of CFRP, Composites B 191 (2020) 107977, http://dx.doi.org/10.1016/j.compositesb.2020.107977.
[44] M. Nakada, Y. Miyano, Accelerated testing for long-term fatigue strength of various FRP laminates for marine use, Compos. Sci. Technol. 69 (6) (2009) 805–813, http://dx.doi.org/10.1016/j.compscitech.2008.02.030.
[45] Y. Miyano, M. Nakada, N. Sekine, Accelerated testing for long-term durability of FRP laminates for marine use, J. Compos. Mater. 39 (1) (2005) 5–20, http://dx.doi.org/10.1177/0021998305046430.
[46] R.M. Guedes, Lifetime predictions of polymer matrix composites under constant or monotonic load, Composites A 37 (5) (2006) 703–715, http://dx.doi.org/10.1016/j.compositesa.2005.07.007.
[47] M.D. Banea, F.S.M. de Sousa, L.F.M. da Silva, R.D.S.G. Campilho, A.M.B. de Pereira, Effects of temperature and loading rate on the mechanical properties of a high temperature epoxy adhesive, J. Adhes. Sci. Technol. 25 (18) (2011) 2461–2474, http://dx.doi.org/10.1163/016942411X580144.
[48] C.C. Hiel, H.F. Brinson, A.H. Cardon, The nonlinear viscoelastic response of resin matrix composites, in: I.H. Marshall (Ed.), Composite Structures 2, Vol. 4, Springer Netherlands, Dordrecht, 1983, pp. 271–281, http://dx.doi.org/10.1007/978-94-009-6640-6_20.
[49] O. Starkova, A. Aniskevich, Application of time-temperature superposition to energy limit of linear viscoelastic behavior, J. Appl. Polym. Sci. 114 (1) (2009) 341–347, http://dx.doi.org/10.1002/app.30528.
[50] R.M. Guedes, Review article: Time-dependent failure criteria for polymer matrix composites: A review, J. Reinf. Plast. Compos. 29 (20) (2010) 3041–3047, http://dx.doi.org/10.1177/0731684410370067.
[51] R.M. Christensen, R.E. Glaser, The application of kinetic fracture mechanics to life prediction for polymeric materials, J. Appl. Mech. 52 (1) (1985) 1–5, http://dx.doi.org/10.1115/1.3168997.
[52] M. Amjadi, A. Fatemi, Creep behavior and modeling of high-density polyethylene (HDPE), Polym. Test. 94 (2021) 107031, http://dx.doi.org/10.1016/j.polymertesting.2020.107031.
[53] X. Duan, H. Yuan, W. Tang, J. He, X. Guan, A phenomenological primary-secondary-tertiary creep model for polymer-bonded composite materials, Polymers 13 (14) (2021) http://dx.doi.org/10.3390/polym13142353.
[54] J. Morais Gautério, L. Cofferri, A.H.M.d.F. da Silva, F. Tempel Stumpf, Lifetime prediction of high-modulus polyethylene yarns subjected to creep using the Larson–Miller methodology, Polym. Polym. Compos. 27 (7) (2019) 400–406, http://dx.doi.org/10.1177/0967391119847534.
[55] O. Starkova, S.T. Buschhorn, E. Mannov, K. Schulte, A. Aniskevich, Water transport in epoxy/MWCNT composites, Eur. Polym. J. 49 (8) (2013) 2138–2148, http://dx.doi.org/10.1016/j.eurpolymj.2013.05.010.
[56] L.R. Grace, Projecting long-term non-fickian diffusion behavior in polymeric composites based on short-term data: A 5-year validation study, J. Mater. Sci. 51 (2) (2016) 845–853, http://dx.doi.org/10.1007/s10853-015-9407-0.
[57] F.X. Perrin, M.H. Nguyen, J.L. Vernet, Water transport in epoxy–aliphatic amine networks – Influence of curing cycles, Eur. Polym. J. 45 (5) (2009) 1524–1534, http://dx.doi.org/10.1016/j.eurpolymj.2009.01.023.
[58] D.T. Hallinan, M.G. de Angelis, M. Giacinti Baschetti, G.C. Sarti, Y.A. Elabd, Non-Fickian diffusion of water in Nafion, Macromolecules 43 (10) (2010) 4667–4678, http://dx.doi.org/10.1021/ma100047z.
[59] M.B. Satterfield, P.W. Majsztrik, H. Ota, J.B. Benziger, A.B. Bocarsly, Mechanical properties of Nafion and titania/Nafion composite membranes for polymer electrolyte membrane fuel cells, J. Polym. Sci. B 44 (16) (2006) 2327–2345, http://dx.doi.org/10.1002/polb.20857.
[60] D. Gibhardt, D. Meyer, L. Braun, C. Buggisch, B. Fiedler, Effects of the hygrothermal aging history on epoxy resins and GFRP composites: Press release in autum 2022, in: Proceedings of the 20th European Conference on Composite Materials, ECCM20, 2022.